

Akt Specific Activator SC79 Protects against Early Brain Injury following Subarachnoid Hemorrhage

Dingding Zhang,[†] Huasheng Zhang,[†] Shuangying Hao,[‡] Huiying Yan,[†] Zihuan Zhang,^{||} Yangchun Hu,[§] Zong Zhuang,[†] Wei Li,[†] Mengliang Zhou,[†] Kuanyu Li,^{*,‡} and Chunhua Hang^{*,†}

[†]Department of Neurosurgery, Jinling Hospital, School of Medicine, Nanjing University, 305 East Zhongshan Road, Nanjing 210002, Jiangsu Province, P. R. China

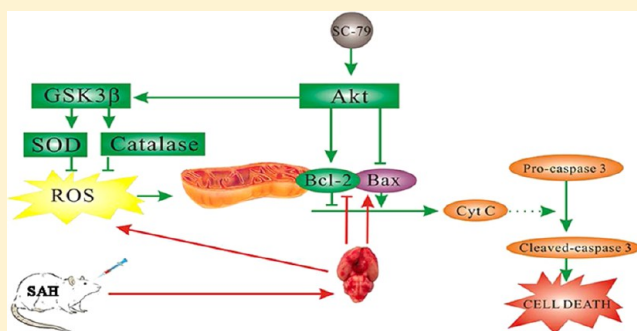
[‡]Jiangsu Key Laboratory for Molecular Medicine, Medical School of Nanjing University, 22 Hankou Road, Nanjing 210093, Jiangsu Province, P. R. China

[§]Department of Neurosurgery, The First Affiliated Hospital of Anhui Medical University, Hefei, Anhui 230031, P. R. China

^{||}Department of Neurosurgery, Jinling Hospital, School of Medicine, Second Military Medical University, Shanghai 200433, China

ABSTRACT: A growing body of evidence demonstrates that Akt may serve as a therapeutic target for treatment of early brain injury following subarachnoid hemorrhage (SAH). The purpose of the current study was to evaluate the neuroprotective effect of Akt specific activator SC79 in an experimental rat model of SAH. SAH was induced by injecting 300 μ L of blood into the prechiasmatic cistern. Intracerebroventricular (ICV) injection of SC79 (30 min post-SAH) induced the p-Akt (Ser473) expression in a dose-dependent manner. A single ICV dose treatment of SC79 (100 μ g/rat) significantly increased the expression of Bcl-2 and p-GSK-3 β (Ser9), decreased the protein levels of Bax, cytoplasm cytochrome *c*, and cleaved caspase-3, indicating the antiapoptotic effect of SC79. As a result, the number of apoptotic cells was reduced 24 h post SAH. Moreover, SC79 treatment alleviated SAH-induced oxidative stress, restored mitochondrial morphology, and improved neurological deficits. Strikingly, treatment of SC79 provided a beneficial outcome against neurologic deficit with a therapeutic window of at least 4 h post SAH by ICV injection and 30 min post SAH by intraperitoneal injection. Collectively, SC79 exerts its neuroprotective effect likely through the dual activities of antioxidation and antiapoptosis. These data provide a basic platform to consider SC79 as a novel therapeutic agent for treatment of SAH.

KEYWORDS: Subarachnoid hemorrhage, early brain injury, Akt, SC79, antioxidation, antiapoptosis



Subarachnoid hemorrhage (SAH) is a common and frequently life-threatening condition with an approximate worldwide incidence of 6–7 per 100 000 persons/year.¹ Accumulating evidence suggests that early brain injury (EBI), which occurs within the first 72 h after SAH, plays a pivotal role in the high mortality and morbidity after SAH; effective treatment against EBI has become a major goal in SAH patient care.^{2,3} Unfortunately, treatment options are limited, as no approved pharmacological therapeutic intervention has been identified thus far. A growing body of evidence suggests that Akt plays an important role in neuronal survival by modulating oxidative and apoptotic processes.^{4–7} Importantly, a number of experimental studies have demonstrated that the acute activation of Akt in the brain confers protection against EBI^{8–12} and deactivation of Akt contributes to pathogenesis of EBI.¹³ These results indicate that elevating Akt activity is a valid target for therapeutic intervention following SAH. In spite of many promising therapeutics showing Akt activation and beneficial effects in animal models of SAH, most elevating Akt signaling drugs have not translated into

clinically effective therapies. This endeavor has been hindered likely due to the lack of specific Akt activators.

The activation of Akt is initiated by membrane recruitment via interaction of its pleckstrin homology domain with phosphatidylinositol 3,4,5-trisphosphate synthesized by phosphoinositide 3-kinase from phosphatidylinositol 4,5-bisphosphate. After membrane anchoring, Akt can then be phosphorylated by its activating kinases, phosphoinositide dependent kinase 1 (at threonine308) and the mammalian target of rapamycin complex 2 (at serine473).¹⁴ Upon phosphorylation, Akt translocates from the plasma membrane to intracellular compartments, including the cytoplasm and nucleus, where it phosphorylates a variety of substrates.¹⁵ SC79 is a unique specific Akt activator that inhibits Akt membrane translocation, but paradoxically activates Akt in the cytosol.¹⁶ Moreover, SC79 has been demonstrated to suppress excitotoxicity and alleviate stroke-induced neuronal

Received: November 23, 2015

Accepted: March 16, 2016

Published: March 16, 2016

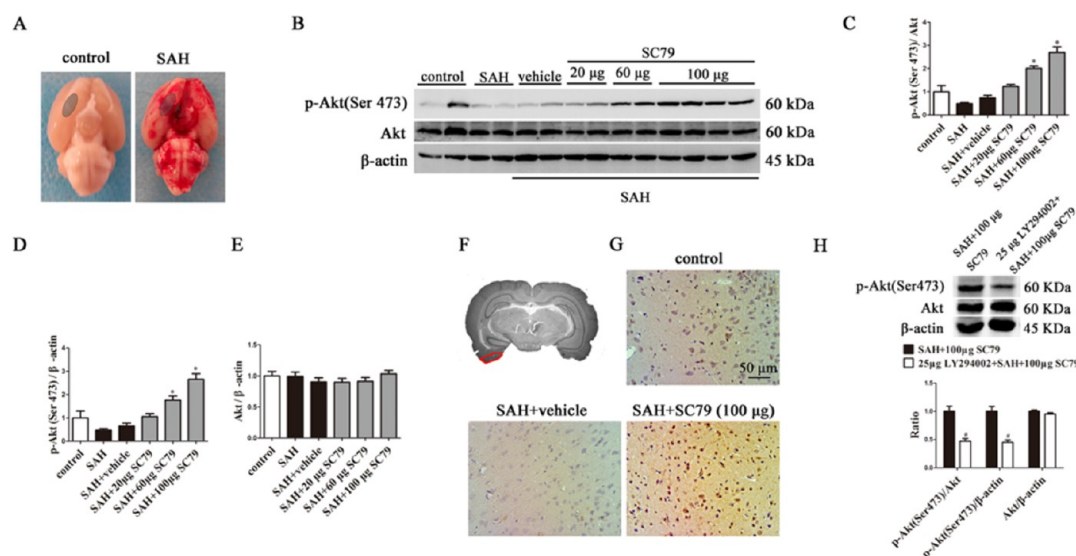


Figure 1. SC79 upregulated p-Akt (Ser473) expression in a dose dependent manner. Western blot analysis to detect the protein levels of total (Akt) and phosphorylated (p-Akt, Ser473) Akt following treatment of SC79 (ICV 30 min post SAH) in basal temporal lobe 24 h after SAH. β -actin was used as the loading control. Quantification analysis showed that SC79 treatment induced p-Akt expression in a dose-dependent manner. Furthermore, pretreatment with Akt selective inhibitor LY294002 (25 μ g/rat) blocked SC79 (100 μ g/rat)-induced p-Akt activation (H). (A) Schematic diagram showing the regions taken for the biochemical assays. (B) Representative Western blotting results for protein levels of Akt and p-Akt. (C–E) Quantitative ratio of p-Akt/Akt, p-Akt/ β -actin, and Akt/ β -actin. (F) Schematic diagram showing the regions taken for the histological assays. (G) Representative immunohistochemical images showing the levels of p-Akt. Data are expressed as mean \pm SEM; * P < 0.05 versus vehicle-treated SAH rats (C–E); # P < 0.05 versus SC-79 treated SAH rats (H), n = 6 in each group.

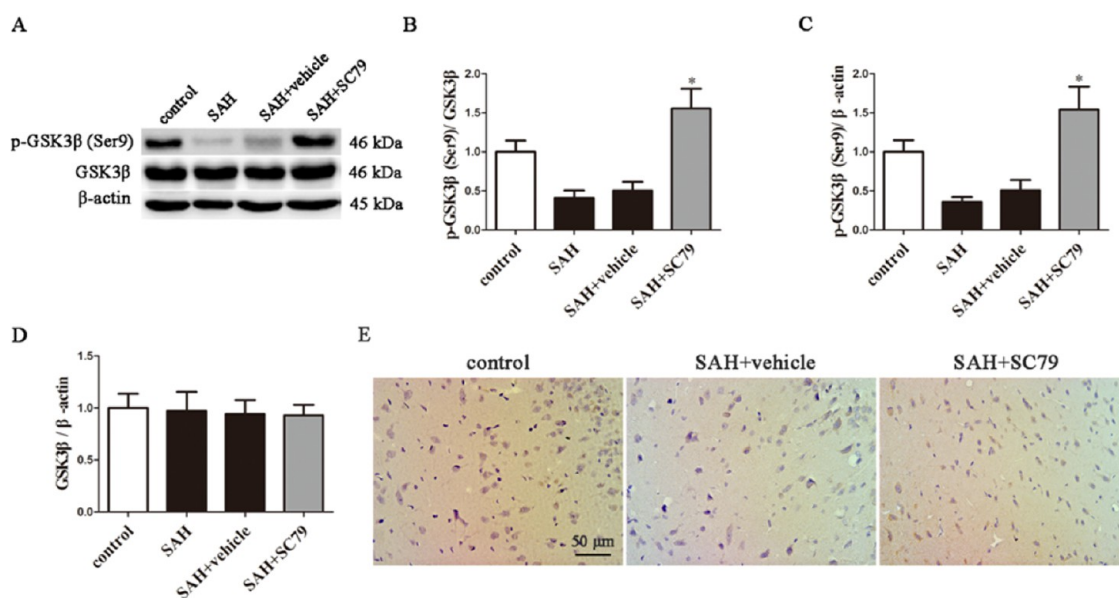


Figure 2. Effects of SC79 treatment on p-GSK3 β (Ser9) expression 24 h after SAH. (A) Representative images of Western blots to detect the protein levels of total and p-GSK3 β (Ser9) in basal temporal lobe following SC79 treatment (ICV 100 μ g/rat 30 min post SAH) at 24 h. β -Actin was used as the loading control. Quantification analysis of Western blots (B–D) showed that p-GSK3 β expression significantly increased in SC79-treated SAH rats compared to the vehicle-treated rats. (E) Representative immunohistochemical images showing the protein levels of p-GSK3 β . Data are expressed as mean \pm SEM; * P < 0.05 versus vehicle-treated SAH rats, n = 6 in each group.

death,¹⁶ indicating that SC79 can be used as a chemical platform to develop novel drugs for neurological complications. In view of the above facts, we evaluated the therapeutic potential and possible mechanism of SC79 in treatment of SAH.

RESULTS AND DISCUSSION

General Observation. Significant variation in body temperature, blood gas, and blood glucose examination was not found

among the experimental groups (data not shown). The mortality rate of rats was 0% (0/67 rats) in the control group and 20.2% (51/252 rats) in SAH groups. All animals in the study tolerated the insertion of the needle and intracerebroventricular (ICV) injection well.

The Akt/Glycogen Synthase Kinase 3 β (GSK3 β) Signaling Pathway Was Activated by SC79 Treatment following SAH. To determine the capability of SC79 to induce p-Akt expression, 20, 60, or 100 μ g of SC79 was ICV administered 30

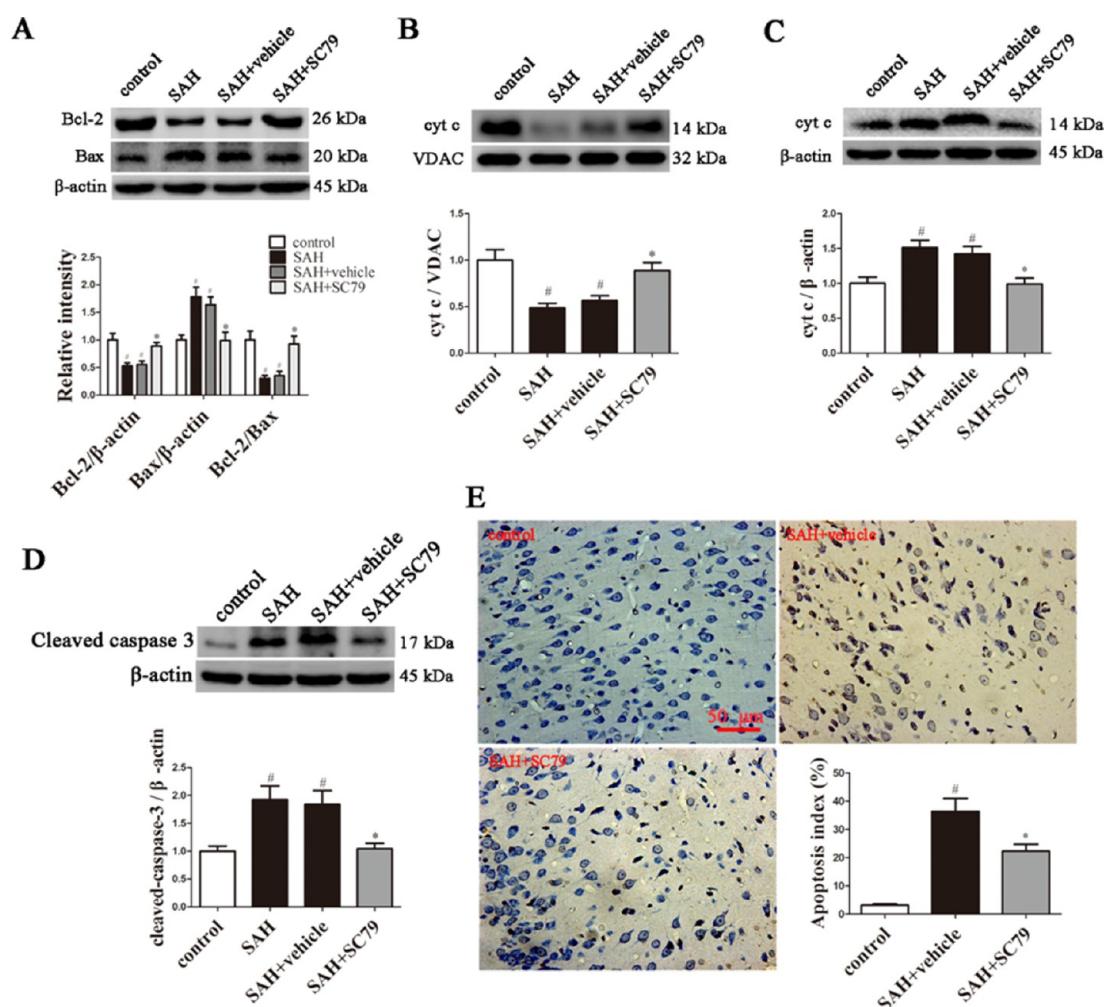


Figure 3. SC79 treatment attenuated SAH-induced apoptosis at 24 h after SAH. Representative immunoblots showing the protein levels of Bcl-2 and Bax (A), mitochondrial (B) and cytosolic (C) cyt *c*, and cleaved caspase-3 (D) in the basal temporal lobe from control, SAH, vehicle-treated, and SC79-treated rats at 24 h post SAH. Bar graphs are the quantitative densitometry of the bands on the immunoblots. (E) Representative TUNEL staining of brain sections of SC79-treated and vehicle-treated rats at 24 h postinjury. Quantification showed that SC79-treated rats had significantly fewer TUNEL positive cells at 24 h than the vehicle-treated rats. Data are expressed as mean \pm SEM; #*P* < 0.05 versus control, **P* < 0.05 versus vehicle-treated SAH rats, *n* = 6 in each group.

min post SAH. The rats were sacrificed 24 h later, and Western blot analysis was performed to examine the expression of p-Akt in the brain (Figure 1). Our result showed that SC79 administration increased the expression of p-Akt in a dose-dependent manner without any obvious changes of the total Akt level (Figure 1B–E). Immunohistochemical assays confirmed that 100 μ g of SC79 markedly increased p-Akt staining compared to vehicle-treated SAH rats (Figure 1G). Because no severe complications were observed at the highest dose (100 μ g) tested, the dose was then chosen to examine its neuroprotective effects on EBI following SAH. Notably, our data also showed that pretreatment with LY294002, a selective inhibitor of Akt,¹⁷ could quench SC79-induced p-Akt expression (Figure 1H), confirming the selectivity of SC79 on Akt activation.

Upon activation through phosphorylation, Akt will translocate from the plasma membrane to intracellular compartments, including the cytoplasm and nucleus, where it phosphorylates a variety of substrates. One of these substrates is GSK3 β , which is inhibited through phosphorylation at serine9 by Akt.¹⁸ We thus examined the phosphorylation of GSK3 β . Western blot and IHC analysis showed that expression of p-GSK3 β (Ser9) in the

cerebral cortex was significantly increased in the SC79-treated animals compared with the vehicle-treated animals 24 h after SAH (Figure 2). These results demonstrated that the Akt/GSK3 β signaling cascade was activated by SC79.

SC79 Treatment Reduced Apoptosis after SAH. Overexpression of active Akt has been shown to reduce neuronal apoptosis following SAH via modulating the expression levels of Bcl-2 and Bax;^{10,19} we therefore explored the possibility and mechanism that SC79 reduced apoptosis after SAH. In line with previous reports,²⁰ both the expression of Bcl-2 and Bcl-2/Bax ratio were significantly decreased in the SAH- and SAH+vehicle-treated groups at 24 h after SAH. However, they markedly increased in SC79-treated SAH rats compared with the SAH- and SAH+vehicle-treated groups (Figure 3A). It is well-known that down-regulation of the Bcl-2/Bax ratio will enhance mitochondrial cytochrome *c* (cyt *c*) release, which will initiate the apoptotic process following SAH.²⁰ Therefore, subcellular fractionation was performed to isolate mitochondrial and cytosolic fractions. Western results demonstrated that SAH-stimulated elevation of cytosolic cyt *c* was reversed by SC79

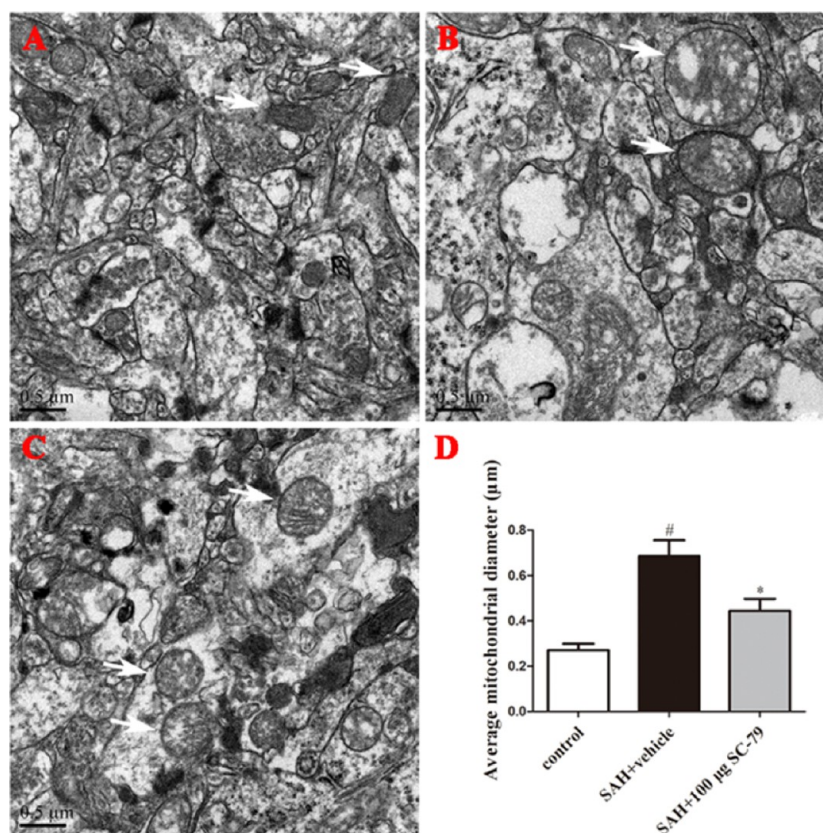


Figure 4. Effect of SC79 treatment on mitochondrial morphology. Four rats in each group were chosen for morphometric analysis at 24 h after SAH. Representative images are presented here. (A) Mitochondria from the control group showing condensed matrix and preserved cristae architectures (see white arrows). (B) Mitochondria from the vehicle treated SAH rat exhibiting abnormal swollen mitochondria with disrupted cristae. (C) Mitochondria from the SC79 treated SAH rat exhibiting obviously improved cristae structure. (D) Quantitation of average mitochondrial diameter showed that SC79 significantly reduced the diameter of mitochondria as compared with vehicle-treated SAH rats. [#] $P < 0.05$ versus control, ^{*} $P < 0.05$ versus vehicle-treated SAH rats.

administration (Figure 3B and C), suggesting that SC79 provides the protection against the initiation of apoptosis.

Once in the cytosol, *cyt c* interacts with its adaptor molecule, Apaf-1, resulting in the recruitment, processing, and activation of pro-caspase-9 in the presence of dATP or ATP.²¹ Caspase-9, in turn, cleaves and activates pro-caspase-3 which results in neuronal apoptosis. To see the end point against the apoptosis by SC79, we further checked the cleaved-caspase-3 and counted the terminal deoxynucleotidyl transferase dUTP nick end labeling (TUNEL) positive cells. The results showed that the level of cleaved caspase-3 was elevated in the SAH groups and reduced after treatment with SC79 (Figure 3D). The number of TUNEL-positive cells was diminished by SC79 administration following SAH (Figure 3E). In support of this mechanism, our data provided consistent results in rat SAH model with the data in other models.^{8–10} Based on the current study, we hypothesized that SC79 exerts its neuroprotective effects, partially, through the antiapoptotic pathways by blocking *cyt c* release from mitochondria.

SC79 Treatment Reduced SAH-Induced Oxidative Stress. Mitochondria disruption, the increased production of reactive oxygen species (ROS), and disruption of the intrinsic antioxidant systems have all been reported in either experimental or human SAH.^{22,23} The surplus ROS will damage the mitochondria, resulting in more production of ROS in a vicious circle. Based on these evidence, we assessed the ability of SC79 to maintain mitochondrial morphology at 24 h post-SAH. As

illustrated in Figure 4A, mitochondria from the cortex in control animals were found to be predominantly regular morphology with condensed cristae. The inflated and vacuolated mitochondria in SAH+vehicle animals were obviously observed 24 h after injury in the basal temporal lobe (Figure 4B). However, SC79 treatment significantly improved mitochondrial morphology (Figures 4C and 4D). In line with these data, it was reported that Akt activation could protect from injury via modulating mitochondrial morphology.²⁴

Given the link between dynamic changes in mitochondrial morphology and production of ROS, we sought to determine whether SC79 could prevent from ROS overproduction in the brain tissue of SAH rats. Our data showed that SC79 significantly reduced the SAH-induced production of ROS (Figure 5A). A previous study has also demonstrated that inhibition of GSK3 β recovers the ROS scavenging enzyme superoxide dismutase (SOD) 1 and catalase levels and, strikingly, induces SOD2 expression in oxygen-deprived neurons.²⁵ Considering the evidence, we determined the protein levels of SOD 1 and 2 and catalase using Western blot analysis. Our results demonstrated that SC79 treatment clearly elevated the protein levels of SOD1, SOD2, and catalase (Figure 5B–D). Moreover, the activities of SOD and catalase significantly increased (Figure 5E and F). These data demonstrated that SC79 treatment significantly evoked a strong defense to scavenge ROS. Consistent with our data, it has been demonstrated that Akt/GSK3 β pathway may partially protect the neuron against cellular

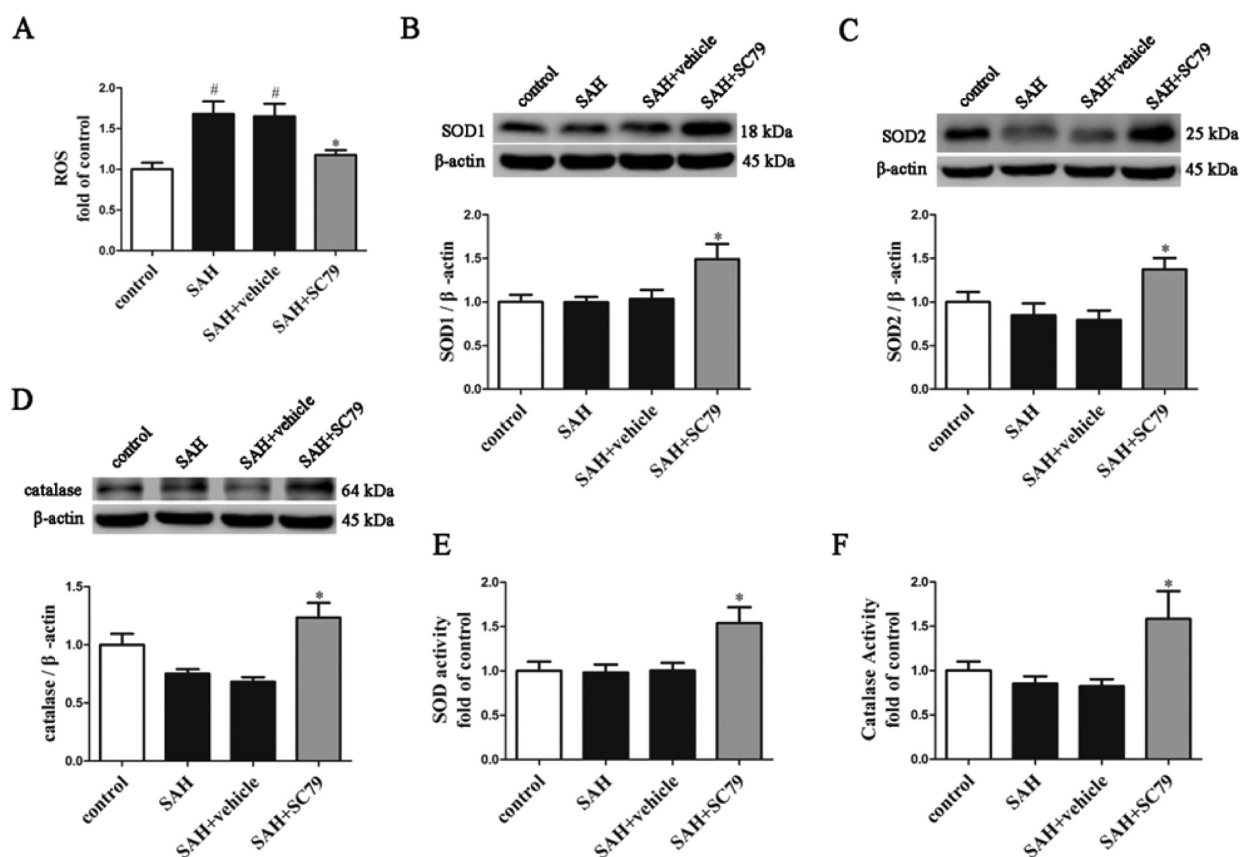


Figure 5. SC79 treatment stimulated the defense against oxidative stress. (A) Treatment of SC79 (100 μ g/rat) significantly reduced SAH-induced ROS levels. (B–D) Western blot analysis presenting the protein levels of SOD1 (B), SOD2 (C), and catalase (D) in control, SAH, and vehicle- and SC79-treated groups. The lower panels are the quantitative data, showing significantly increased protein levels of SOD1, SOD2, and catalase after SC79 treatment. Moreover, SC79 treatment upregulated the activities of SOD (E) and catalase (F). Data are expressed as mean \pm SEM, [#] $P < 0.05$ versus control, ^{*} $P < 0.05$ versus vehicle-treated SAH rats, $n = 6$ in each group.

oxidant generation.^{25,26} It has also been proved that pharmacological GSK-3 β inhibitors replenish the antioxidant capacity and restores mitochondrial bioenergetics.²⁵ Hence, it is speculated that the suppression of oxidative stress by activating Akt/GSK3 β signaling contributes to the neuro-protective effects of SC79.

SC79 Treatment Promoted Behavioral Recovery and Neuronal Survival following SAH. Based on the neuro-protective properties of SC79 documented above, we assessed the efficacy of SC79 treatment on functional recovery after SAH (Figure 6A and B). The vehicle-treated SAH rats showed statistically significantly neurological behavior impairment at 24 and 72 h when compared with control group (Figure 6A). However, when treated with SC79 (30 min post-SAH), the rats showed remarkable improvement of neurological defect (Figure 6A, see SAH+SC79 group). For a therapeutic compound to be considered clinically relevant, we provided a delayed window post SAH to treat the rats with SC79 using a separate cohort of rats. As shown in Figure 6B, such treatment resulted in a very similar consequence to when given 30 min post SAH; that is, SC79 significantly improved neurological deficit when given 4 h after SAH, which suggests its clinical potential. To further verify whether the efficacy of SC79 treatment represents the increase of neuronal survival after SAH, tissue sections (3 days post-SAH group) were stained with Cresyl Violet. The data showed considerable neuronal loss in the cortex 3 days after SAH (Figure 6C and D), where loss, importantly, was significantly attenuated by either acute or delayed administration of a single dose of SC79. Considering that SC79 has been previously reported to

cross the blood-brain barrier after intraperitoneal (IP) injection,¹⁶ we further investigated whether these same neuro-protective effects of SC79 can be observed when IP injection. Our data demonstrated that IP injection of SC79 could also significantly improve the neurological deficits and reduced neuronal damage (Figure 7). This finding further suggests a clinical rationale for the therapeutic treatment of patients suffering from SAH.

SUMMARY AND CONCLUSIONS

Collectively, our results provide the first evidence that Akt specific activator SC79 is an effective reagent for SAH treatment in a rat model. The neuroprotective effects of SC79 were preserved even when first administered at 4 h post-SAH. The mechanism of the neuroprotective effect is most likely due to the ability of SC79 to reduce SAH-induced oxidative stress and apoptosis as illustrated in Figure 8. Our results suggest a therapeutic rationale of SC79 for treatment of clinical SAH.

METHODS

Animals and SAH Model. The male Sprague–Dawley rats weighing 300–350 g were used in this study. Rats were housed in a reversed 12 h light/12 h dark cycle controlled environment with free access to food and water. All experimental protocols involving animals were approved by Nanjing University Animal Care and Use Committee and in accordance with the Guide for the Care and Use of Laboratory Animals by the National Institute of Health.

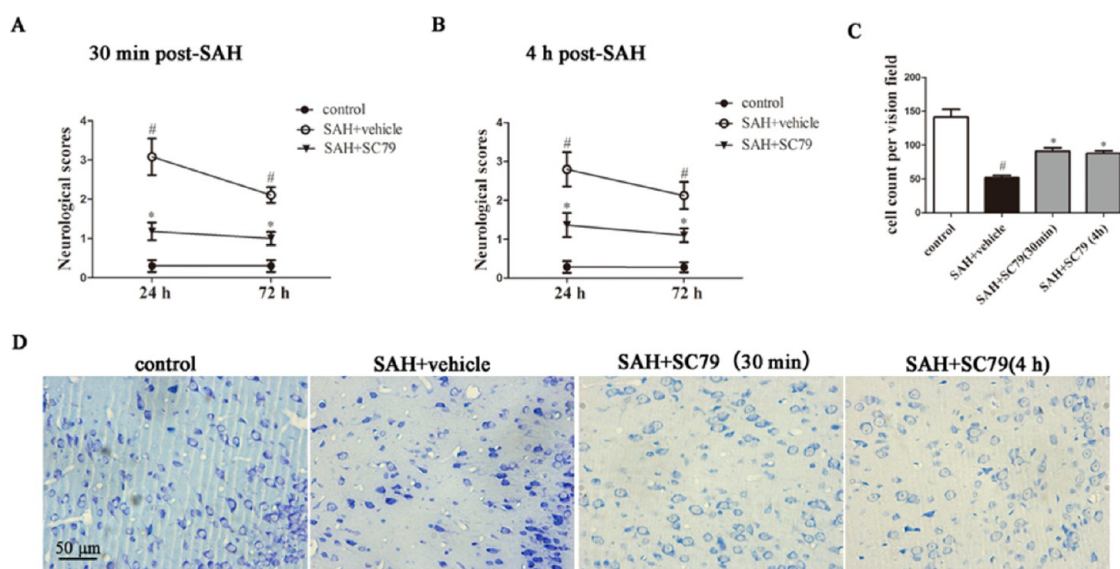


Figure 6. Effect of SC79 (100 μg , ICV) treatment on neurological deficits and neuronal survival after SAH. Adult male rats were subjected to sham injury (control) or SAH and received an ICV injection of vehicle or 100 μg of SC79. (A) SC79 treatment (30 min post SAH) significantly decreased the neurological scores at both 24 and 72 h post SAH. Numbers of the rats in each group are as follows: control, $n = 10$; SAH+vehicle, 24 h, $n = 12$; 72 h, $n = 9$; SAH+SC79, 24 h, $n = 11$; 72 h, $n = 9$. (B) Neurologic deficits were significantly alleviated in rats receiving SC79 treatment 4 h post SAH, compared to vehicle-treated rats at 24 and 72 h post-SAH. Numbers of the rats in each group are as follows: control, $n = 8$; SAH+vehicle (24 h, $n = 10$; 72 h, $n = 8$) and SAH+SC79 (24 h, $n = 11$; 72 h, $n = 10$). $\#P < 0.05$ versus control, $*P < 0.05$ versus vehicle. (C) Quantitative numbers of the survived neurons counted at 72 h postinjury after Cresyl Violet staining. (D) Representative images of Cresyl Violet stained brain sections illustrating morphological features of neurons. SC79 treatment attenuated SAH-induced neuronal loss in the cortex compared to the vehicle-treated SAH group at 72 h post-SAH. Data are expressed as mean \pm SEM, $\#P < 0.05$ versus control, $*P < 0.05$ versus vehicle-treated SAH rats, $n = 6$ in each group.

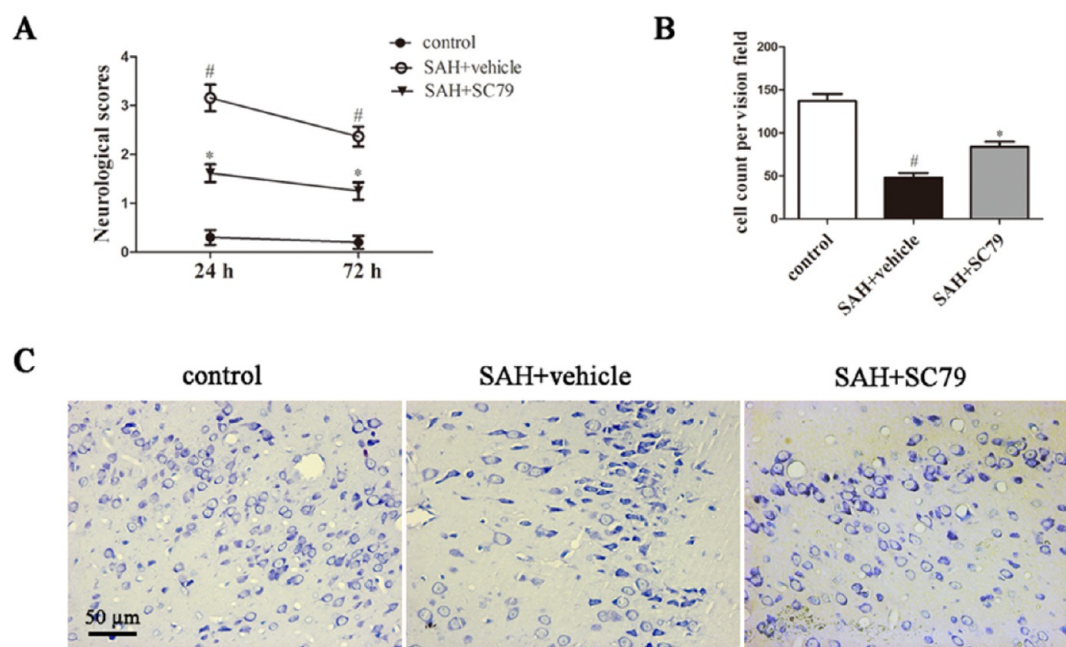


Figure 7. Effect of SC79 (0.04 mg/g, IP) treatment on neurological deficits and neuronal survival after SAH. Adult male rats were subjected to sham injury (control) or SAH and received a single IP injection of vehicle or 0.04 mg/g of SC79 at 30 min after SAH. (A) SC79 treatment significantly decreased the neurological scores at both 24 and 72 h post SAH. Numbers of the rats in each group are as follows: control, $n = 10$; SAH+vehicle, 24 h, $n = 13$; 72 h, $n = 11$; SAH+SC79, 24 h, $n = 13$; 72 h, $n = 12$. (B) Quantitative numbers of the survived neurons counted at 72 h postinjury after cresyl violet staining. (C) Representative images of cresyl violet stained brain sections illustrating morphological features of neurons. SC79 treatment attenuated SAH-induced neuronal loss in the cortex compared to the vehicle-treated SAH group at 72 h post-SAH. Data are expressed as mean \pm SEM, $\#P < 0.05$ versus control, $*P < 0.05$ versus vehicle-treated SAH rats, $n = 6$ in each group.

Experimental SAH was performed as described previously in our laboratory and other laboratories.^{27–30} Briefly, the rats were intraperitoneally anesthetized with 10% chloral hydrate (400 mg/kg body weight) and placed in a stereotaxic head frame. An insulin injection

needle (BD Science) was tilted 45° in the sagittal plane, and placed 8 mm anterior to bregma in the midline, with the hole facing the right side. It was lowered until the tip reached the base of the skull, 2–3 mm anterior to the chiasma (approximately 10–12 mm from the brain

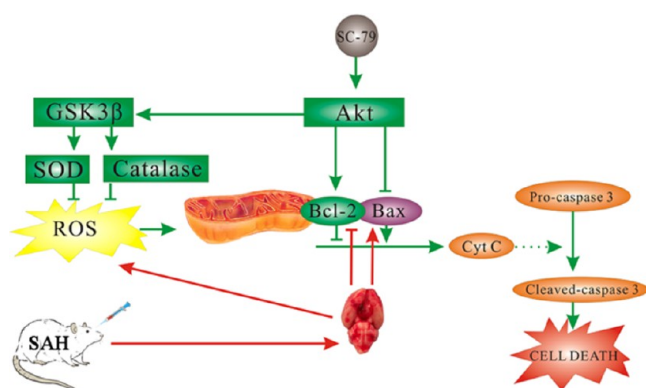


Figure 8. Schematic representation for the proposed mechanism of neuroprotection of SC79 from SAH-induced injury. SC79 stimulates Akt activation, which inhibits GSK3 β activation, and upregulates the expression of SOD1, SOD2, and catalase and their activities, resulting in removal of ROS and preservation of mitochondrial morphology. Akt also increases Bcl-2/Bax ratio to prevent the release of cyt *c* and caspase-3 cleavage and, therefore, protects cells from apoptosis.

surface) and retracted 0.5 mm. Loss of cerebrospinal fluid and bleeding from the midline vessels were prevented by plugging the burr hole with bone wax before inserting the needle. A total of 300 μ L nonheparinized fresh autologous arterial blood was slowly injected into the prechiasmatic cistern for 3 min under aseptic technique. The heart rate was monitored and the rectal temperature was kept at 37 ± 0.5 °C by using physical cooling (ice bag) when required throughout experiments. Arterial blood samples were analyzed intermittently to maintain pO₂, pCO₂, and pH, parameters within normal physiological ranges. To maintain fluid balance, all rats were supplemented with 2 mL of 0.9% NaCl administered subcutaneously. After recovering from anesthesia, rats were returned to their cages with free-access food and water provided ad libitum. In the present study, we observed that the basal temporal lobe was always stained with blood as described before. Therefore, the brain tissue adjacent to the clotted blood was used for analysis in our study. The saline control group underwent injection of 300 μ L of 0.9% NaCl into the subarachnoid space.

Study Design 1. SC79 was purchased from Sigma-Aldrich (St. Louis, MO) and freshly prepared in dimethyl sulfoxide (DMSO) just before ICV injection. In our dose–response study, we tested different dosages at 20, 60, and 100 μ g. SC79 solution or DMSO (5 μ L) was injected into the left lateral ventricle 30 min post SAH using a 10 μ L Hamilton microsyringe. ICV injection was performed according to our previous study.³¹ Then, the rats were sacrificed 24 h after SAH for the biochemical and histological analysis. The rats were randomly assigned to following groups: (1) Control group ($n = 39$); (2) SAH group ($n = 40$); (3) SAH + vehicle group ($n = 49$); (4) SAH + 20 μ g SC79 group ($n = 8$); (5) SAH + 60 μ g SC79 group ($n = 10$) and (6) SAH + 100 μ g SC79 group ($n = 48$). Of them, 9 rats with SAH were excluded later from the study because of little blood in prechiasmatic cistern but lots of blood clot in the frontal lobe instead, and 26 (SAH, $n = 7$; SAH + vehicle, $n = 8$; SAH + 20 μ g SC79, $n = 2$; SAH + 60 μ g SC79, $n = 2$; SAH + 100 μ g SC79, $n = 7$) SAH rats died before sacrifice. In another experiment, seven rats were pretreated with LY294002, a selective inhibitor of Akt,¹⁷ followed by SC79 treatment (ICV 30 min after SAH). The dosage of LY294002 which used in the current study was selected based on previous studies.^{12,32} One SAH rat died before sacrifice.

A separate group of rats was followed for 72 h functional testing after which brain tissue was collected for histological assessment. We used 40 animals in this study, assigned to following groups: (1) Control group ($n = 10$); (2) SAH + vehicle group ($n = 16$), and (3) SAH + 100 μ g SC79 group ($n = 14$). Three rats with SAH were excluded because of blood clot in the frontal lobe. Nine (SAH + vehicle, $n = 5$; SAH + 100 μ g SC79, $n = 4$) SAH rats died before the intended sacrifice. A total of 241 rats were used in study 1.

Study Design 2. To evaluate the neuroprotective potential of SC79 against SAH-induced neurological deficits, we used a delayed and more clinically relevant treatment paradigm in which SC79 or DMSO was administered by ICV injection at 4 h post-SAH. Then the rats were functionally tested after 3 days and the brain tissue was collected for histological assessment. We used 38 animals in this study, assigned to following groups: (1) Control group ($n = 8$); (2) SAH + vehicle group ($n = 15$), and (3) SAH + 100 μ g SC79 group ($n = 15$). Four rats with SAH were excluded because of blood clot in the frontal lobe. Eight (SAH + vehicle, $n = 5$; SAH + 100 μ g SC79, $n = 3$) SAH rats died before sacrifice.

Study Design 3. To evaluate the drug with more clinical relevance, rats were treated with SC79 with a single dose of SC79 (0.04 mg/g) via IP injection at 30 min after SAH. The dosage was selected based on previous study.¹⁶ The rats were functionally tested after 3 days and the brain tissue was collected for histological assessment. A total of 40 rats were used in this experiment. Details are as follows: (1) Control group ($n = 10$); (2) SAH + vehicle group (DMSO, $n = 15$); (3) SAH + SC79 group (0.04 mg/g, $n = 15$). Seven (SAH + vehicle, $n = 4$; SAH + 0.04 mg/g SC79 group, $n = 3$) SAH rats died before sacrifice.

Biochemical Analysis. Figure 1A shows the schematic diagram of regions taken for the biochemical assays. The whole cell lysates, mitochondrial and cytosolic extracts were prepared according to the methods described previously. For Western blot analysis, 40 μ g of total protein was loaded in each lane of SDS-PAGE, electrophoresed, and transferred to a nitrocellulose membrane. The blot containing the transferred protein was blocked in blocking buffer (1 \times Tris-buffered saline with Tween 20 with 5% w/v nonfat dry milk without antibody) for 1 h at room temperature followed by overnight primary antibody incubation at 4 °C. The primary antibody was against Akt, p-Akt (Ser473), GSK3 β , p-GSK3 β (Ser9), cleaved-caspase-3, VDAC, cyt *c*, or β -actin (1:1000; from Cell Signaling Technology, Danvers, MA), Bcl-2 and catalase (1:200; from Santa Cruz Biotech., Santa Cruz, CA), SOD1 (1:200; from Boster, Wuhan, China), and SOD2 (1:1000; Abcam, Cambridge, MA). Signal was detected with horseradish peroxidase-conjugated immunoglobulin G (IgG) using enhanced chemiluminescence detection reagents (Millipore Corporation, Billerica, MA). Blot bands were quantified by densitometry with ImageJ software.

Basal temporal lobe tissues were collected 24 h after SAH for measurement of SOD and catalase activities. The Total Superoxide Dismutase Assay Kit with WST-8 (cat # S0101, Beyotime, Nantong, China) and Catalase Assay Kit (visible light) (cat # A007-1, Nanjing Jiancheng Bioengineering Institute, Nanjing, China) were purchased for enzymatic assays of SOD and catalase, respectively. The assays were conducted according to the manufacturer's instruction.

The ROS Detection Kit (cat # GMS10016.4), purchased from Genmed Scientifics Inc., was used to determine the cellular ROS levels. All procedures were performed according to the manufacturer's protocol.

Histological Examination. Figure 1F shows the schematic diagram of regions taken for the histological assays. Rats were anesthetized and transcardially perfused with saline and 4% paraformaldehyde. The brains were removed and postfixed in paraformaldehyde for 24 h. Immunohistochemistry (IHC) was performed to ascertain the immunoreactivity of p-Akt (Ser473) and p-GSK3 β (Ser9). Briefly, the tissue sections (4 μ m) were deparaffinized and rehydrated in gradient alcohol. And then the sections were incubated with anti-p-Akt (Ser473) and p-GSK3 β (Ser9) antibody (diluted 1:50, Cell Signaling, Danvers, MA) overnight at 4 °C, followed by a 15 min wash in phosphate-buffered saline. After that the sections were incubated with HRP conjugated IgG (diluted 1:500, Santa Cruz Biotech) for 60 min at room temperature. 3,3'-Diaminobenzidine/H₂O₂ solution was used to visualize p-Akt and p-GSK3 β . The specificity of the IHC reaction was evaluated by replacement of the primary antibody with rabbit IgG.

TUNEL assay was conducted by using a TUNEL detection kit (In situ Cell Death Detection Kit, Roche Applied Science) according to the manufacturer's instructions and our previous study.³¹ The positive cells were identified, counted, and analyzed under the light microscope by an investigator blinded to the grouping. The extent of brain damage was evaluated by the apoptotic index, defined as the average percentage of TUNEL-positive cells in each section counted in 10 cortical microscopic

fields (at $\times 400$ magnification). Five sections spaced a minimum of 100 μm apart were obtained from each animal and used for quantification. The final average percentage of apoptotic index of the five sections was regarded as the data for each sample.

Formalin-fixed brains (72 h post-SAH) were dehydrated, embedded in paraffin, and sliced into 4 μm thick sections which were stained with Cresyl Violet as described before.^{30,31} The sampled region for each subfield was demarcated in the basal temporal lobe and cresyl-violet neuronal cell bodies were counted. Normal neurons have relatively big cell bodies with light-stained cytoplasm and large and round nuclei. In contrast, damaged cells show shrunken cell bodies, condensed nuclei and dark-stained cytoplasm.^{30,33} To quantify the amount of Nissl staining, the averages of 10 different fields of view were calculated for each animal and the mean number of intact neurons in the ten views was regarded as the data of each section. A total of five sections (with a minimum of 100 μm from the next) from each animal were used for quantification. The final average number of the five sections was regarded as the data for each sample.

Mitochondrial morphology was determined using a transmission electron microscopy as described before.²⁹ Four rats in each group were chosen for morphometric analysis at 24 h after SAH. Quantitative assessment of mitochondrial morphology was evaluated by measuring the diameters [(minimal mitochondrial diameter + maximal diameter)/2] of 50 mitochondria per brain. The final average value of the 50 mitochondria was regarded as the diameter for each rat.

Neurologic Scoring. Three behavioral activity examinations to record appetite, activity, and neurological deficits (Table 1) were performed by an investigator blinded to the study groups at 24 and 72 h after SAH using the scoring system reported previously.^{29,34,35}

Table 1. Behavior and Activity Scores

category	behavior	score
appetite	finished meal	0
	left meal unfinished	1
	scarcely ate	2
activity	walk and reach at least three corners of the cage	0
	walk with some stimulations	1
	almost always lying down	2
deficits	no deficits	0
	unstable walk	1
	impossible to walk	2

Statistical Analyses. Data are expressed as mean \pm SEM. One-way ANOVA followed by Tukey test was used to analyze differences between groups except for the neurobehavioral scores, which were analyzed with nonparametric tests (Kruskal–Wallis, followed by Dunn's posthoc test). SPSS 16.0 was used for the statistical analysis (SPSS, Inc., Chicago, IL). Differences were determined to be significant with $P < 0.05$.

AUTHOR INFORMATION

Corresponding Authors

*(C.H.) Tel/Fax: +86-25-80863310. E-mail: hang_neurosurgery@163.com.

*(K.L.) E-mail: likuanyu@nju.edu.cn.

Author Contributions

D. Zhang designed the study, performed the SAH model and biochemical analysis, and wrote the manuscript. H. Zhang prepared the drug solutions and performed histological examination. H. Yan, W. Li, and Z. Zhang performed the IHC analyses and the animal studies. S. Hao and Y. Hu contributed to the Western blotting and Nissl staining. Z. Zhuang and M. Zhou designed the animal studies. C. Hang and K. Li contributed to the design and analysis of the study and wrote the manuscript. All authors approved the final version of the manuscript.

Funding

This work was supported by grants from the National Natural Science Foundation of China (NSFC, No. 81371294) and the Natural Science Foundation of Jiangsu Province (No. BK20141375) to C. Hang, NSFC (Nos. 31071085, 31371060) to K. Li, NSFC (No. 81400980) to Z. Zhuang, and NSFC (No. 81401029) to W. Li.

Notes

The authors declare no competing financial interest.

ACKNOWLEDGMENTS

The authors thank Bo Yu for technical support.

ABBREVIATIONS

SAH, subarachnoid hemorrhage; EBI, early brain injury; ICV, intracerebroventricular; IP, intraperitoneal; GSK3 β , glycogen synthase kinase 3 β ; DMSO, dimethyl sulfoxide; TUNEL, terminal deoxynucleotidyl transferase dUTP nick end labeling; IgG, immunoglobulin G; SOD, superoxide dismutase; ROS, reactive oxygen species; IHC, immunohistochemistry; cyt c, cytochrome c; NSFC, National Natural Science Foundation of China

REFERENCES

- (1) van Gijn, J., Kerr, R. S., and Rinkel, G. J. (2007) Subarachnoid haemorrhage. *Lancet* 369, 306–318.
- (2) Caner, B., Hou, J., Altay, O., Fuj, M., and Zhang, J. H. (2012) Transition of research focus from vasospasm to early brain injury after subarachnoid hemorrhage. *J. Neurochem.* 123 (Suppl 2), 12–21.
- (3) Sehba, F. A., Hou, J., Pluta, R. M., and Zhang, J. H. (2012) The importance of early brain injury after subarachnoid hemorrhage. *Prog. Neurobiol.* 97, 14–37.
- (4) Koskimaki, J., Matsui, N., Umemori, J., Rantamaki, T., and Castrén, E. (2015) Nimodipine activates TrkB neurotrophin receptors and induces neuroplastic and neuroprotective signaling events in the mouse hippocampus and prefrontal cortex. *Cell. Mol. Neurobiol.* 35, 189–196.
- (5) Noshita, N., Lewen, A., Sugawara, T., and Chan, P. H. (2002) Akt phosphorylation and neuronal survival after traumatic brain injury in mice. *Neurobiol. Dis.* 9, 294–304.
- (6) Noshita, N., Lewen, A., Sugawara, T., and Chan, P. H. (2001) Evidence of phosphorylation of Akt and neuronal survival after transient focal cerebral ischemia in mice. *J. Cereb. Blood Flow Metab.* 21, 1442–1450.
- (7) Endo, H., Nito, C., Kamada, H., Nishi, T., and Chan, P. H. (2006) Activation of the Akt/GSK3 β signaling pathway mediates survival of vulnerable hippocampal neurons after transient global cerebral ischemia in rats. *J. Cereb. Blood Flow Metab.* 26, 1479–1489.
- (8) Duris, K., Manaenko, A., Suzuki, H., Rolland, W. B., Krafft, P. R., and Zhang, J. H. (2011) $\alpha 7$ nicotinic acetylcholine receptor agonist PNU-282987 attenuates early brain injury in a perforation model of subarachnoid hemorrhage in rats. *Stroke* 42, 3530–3536.
- (9) Altay, O., Hasegawa, Y., Sherchan, P., Suzuki, H., Khatibi, N. H., Tang, J., and Zhang, J. H. (2012) Isoflurane delays the development of early brain injury after subarachnoid hemorrhage through sphingosine-related pathway activation in mice. *Crit. Care Med.* 40, 1908–1913.
- (10) Hong, Y., Shao, A., Wang, J., Chen, S., Wu, H., McBride, D. W., Wu, Q., Sun, X., and Zhang, J. (2014) Neuroprotective effect of hydrogen-rich saline against neurologic damage and apoptosis in early brain injury following subarachnoid hemorrhage: possible role of the Akt/GSK3 β signaling pathway. *PLoS One* 9, e96212.
- (11) Zhou, X. M., Zhou, M. L., Zhang, X. S., Zhuang, Z., Li, T., Shi, J. X., and Zhang, X. (2014) Resveratrol prevents neuronal apoptosis in an early brain injury model. *J. Surg. Res.* 189, 159–165.
- (12) Zhuang, Z., Zhao, X., Wu, Y., Huang, R., Zhu, L., Zhang, Y., and Shi, J. (2011) The anti-apoptotic effect of PI3K-Akt signaling pathway after subarachnoid hemorrhage in rats. *Ann. Clin. Lab. Sci.* 41, 364–372.

- (13) Endo, H., Nito, C., Kamada, H., Yu, F., and Chan, P. H. (2006) Akt/GSK3beta survival signaling is involved in acute brain injury after subarachnoid hemorrhage in rats. *Stroke* 37, 2140–2146.
- (14) Vanhaesebroeck, B., and Alessi, D. R. (2000) The PI3K-PDK1 connection: more than just a road to PKB. *Biochem. J.* 346 (Pt 3), 561–576.
- (15) Fan, C. D., Lum, M. A., Xu, C., Black, J. D., and Wang, X. (2013) Ubiquitin-dependent regulation of phospho-AKT dynamics by the ubiquitin E3 ligase, NEDD4-1, in the insulin-like growth factor-1 response. *J. Biol. Chem.* 288, 1674–1684.
- (16) Jo, H., Mondal, S., Tan, D., Nagata, E., Takizawa, S., Sharma, A. K., Hou, Q., Shanmugasundaram, K., Prasad, A., Tung, J. K., Tejada, A. O., Man, H., Rigby, A. C., and Luo, H. R. (2012) Small molecule-induced cytosolic activation of protein kinase Akt rescues ischemia-elicited neuronal death. *Proc. Natl. Acad. Sci. U. S. A.* 109, 10581–10586.
- (17) Vlahos, C. J., Matter, W. F., Hui, K. Y., and Brown, R. F. (1994) A specific inhibitor of phosphatidylinositol 3-kinase, 2-(4-morpholinyl)-8-phenyl-4H-1-benzopyran-4-one (LY294002). *J. Biol. Chem.* 269, 5241–5248.
- (18) Toker, A. (2000) Protein kinases as mediators of phosphoinositide 3-kinase signaling. *Mol. Pharmacol.* 57, 652–658.
- (19) Hasegawa, Y., Suzuki, H., Sozen, T., Altay, O., and Zhang, J. H. (2011) Apoptotic mechanisms for neuronal cells in early brain injury after subarachnoid hemorrhage. *Acta Neurochir Suppl* 110, 43–48.
- (20) Chen, J., Wang, L., Wu, C., Hu, Q., Gu, C., Yan, F., Li, J., Yan, W., and Chen, G. (2014) Melatonin-enhanced autophagy protects against neuronal apoptosis via a mitochondrial pathway in early brain injury following a subarachnoid hemorrhage. *J. Pineal Res.* 56, 12–19.
- (21) D'Amelio, M., Cavallucci, V., and Cecconi, F. (2010) Neuronal caspase-3 signaling: not only cell death. *Cell Death Differ.* 17, 1104–1114.
- (22) Ersahin, M., Toklu, H. Z., Cetinel, S., Yuksel, M., Yegen, B. C., and Sener, G. (2009) Melatonin reduces experimental subarachnoid hemorrhage-induced oxidative brain damage and neurological symptoms. *J. Pineal Res.* 46, 324–332.
- (23) Munakata, A., Ohkuma, H., Nakano, T., Shimamura, N., Asano, K., and Naraoka, M. (2009) Effect of a free radical scavenger, edaravone, in the treatment of patients with aneurysmal subarachnoid hemorrhage. *Neurosurgery* 64, 423–428 discussion 428–429.
- (24) Ong, S. B., Hall, A. R., Dongworth, R. K., Kalkhoran, S., Pyakurel, A., Scorrano, L., and Hausenloy, D. J. (2015) Akt protects the heart against ischaemia-reperfusion injury by modulating mitochondrial morphology. *Thromb. Haemostasis* 113, 513–521.
- (25) Valerio, A., Bertolotti, P., Delbarba, A., Perego, C., Dossena, M., Ragni, M., Spano, P., Carruba, M. O., De Simoni, M. G., and Nisoli, E. (2011) Glycogen synthase kinase-3 inhibition reduces ischemic cerebral damage, restores impaired mitochondrial biogenesis and prevents ROS production. *J. Neurochem.* 116, 1148–1159.
- (26) Uranga, R. M., Katz, S., and Salvador, G. A. (2013) Enhanced phosphatidylinositol 3-kinase (PI3K)/Akt signaling has pleiotropic targets in hippocampal neurons exposed to iron-induced oxidative stress. *J. Biol. Chem.* 288, 19773–19784.
- (27) Chen, G., Li, Q., Feng, D., Hu, T., Fang, Q., and Wang, Z. (2013) Expression of NR2B in different brain regions and effect of NR2B antagonism on learning deficits after experimental subarachnoid hemorrhage. *Neuroscience* 231, 136–144.
- (28) Sabri, M., Ai, J., Lass, E., D'Abbondanza, J., and Macdonald, R. L. (2013) Genetic elimination of eNOS reduces secondary complications of experimental subarachnoid hemorrhage. *J. Cereb. Blood Flow Metab.* 33, 1008–1014.
- (29) Yan, H., Zhang, D., Hao, S., Li, K., and Hang, C. H. (2015) Role of Mitochondrial Calcium Uniporter in Early Brain Injury After Experimental Subarachnoid Hemorrhage. *Mol. Neurobiol.* 52, 1637–1647.
- (30) Zhang, D., Yan, H., Li, H., Hao, S., Zhuang, Z., Liu, M., Sun, Q., Yang, Y., Zhou, M., Li, K., and Hang, C. (2015) TGFbeta-activated Kinase 1 (TAK1) Inhibition by SZ-7-Oxozeanol Attenuates Early Brain Injury after Experimental Subarachnoid Hemorrhage. *J. Biol. Chem.* 290, 19900–19909.
- (31) Zhang, D., Hu, Y., Sun, Q., Zhao, J., Cong, Z., Liu, H., Zhou, M., Li, K., and Hang, C. (2013) Inhibition of transforming growth factor beta-activated kinase 1 confers neuroprotection after traumatic brain injury in rats. *Neuroscience* 238, 209–217.
- (32) Hui, L., Pei, D. S., Zhang, Q. G., Guan, Q. H., and Zhang, G. Y. (2005) The neuroprotection of insulin on ischemic brain injury in rat hippocampus through negative regulation of JNK signaling pathway by PI3K/Akt activation. *Brain Res.* 1052, 1–9.
- (33) Ooigawa, H., Nawashiro, H., Fukui, S., Otani, N., Osumi, A., Toyooka, T., and Shima, K. (2006) The fate of Nissl-stained dark neurons following traumatic brain injury in rats: difference between neocortex and hippocampus regarding survival rate. *Acta Neuropathol.* 112, 471–481.
- (34) Wang, Z., Ma, C., Meng, C. J., Zhu, G. Q., Sun, X. B., Huo, L., Zhang, J., Liu, H. X., He, W. C., Shen, X. M., Shu, Z., and Chen, G. (2012) Melatonin activates the Nrf2-ARE pathway when it protects against early brain injury in a subarachnoid hemorrhage model. *J. Pineal Res.* 53, 129–137.
- (35) Yamaguchi, M., Zhou, C. M., Nanda, A., and Zhang, J. H. (2004) Ras protein contributes to cerebral vasospasm in a canine double-hemorrhage model. *Stroke* 35, 1750–1755.